

# Resting-state Dynamics as a Cortical Signature of Anesthesia in Monkeys

Lynn Uhrig, M.D., Ph.D., Jacobo D. Sitt, M.D., Ph.D., Amaury Jacob, M.Sc., Jordy Tasserie, M.Sc., Pablo Barttfeld, Ph.D., Morgan Dupont, M.Sc., Stanislas Dehaene, Ph.D., Bechir Jarraya, M.D., Ph.D.

## ABSTRACT

**Background:** The mechanism by which anesthetics induce a loss of consciousness remains a puzzling problem. We hypothesized that a cortical signature of anesthesia could be found in an increase in similarity between the matrix of resting-state functional correlations and the anatomical connectivity matrix of the brain, resulting in an increased function-structure similarity.

**Methods:** We acquired resting-state functional magnetic resonance images in macaque monkeys during wakefulness ( $n = 3$ ) or anesthesia with propofol ( $n = 3$ ), ketamine ( $n = 3$ ), or sevoflurane ( $n = 3$ ). We used the k-means algorithm to cluster dynamic resting-state data into independent functional brain states. For each condition, we performed a regression analysis to quantify function-structure similarity and the repertoire of functional brain states.

**Results:** Seven functional brain states were clustered and ranked according to their similarity to structural connectivity, with higher ranks corresponding to higher function-structure similarity and lower ranks corresponding to lower correlation between brain function and brain anatomy. Anesthesia shifted the brain state composition from a low rank (rounded rank [mean  $\pm$  SD]) in the awake condition (awake rank = 4 [3.58  $\pm$  1.03]) to high ranks in the different anesthetic conditions (ketamine rank = 6 [6.10  $\pm$  0.32]; moderate propofol rank = 6 [6.15  $\pm$  0.76]; deep propofol rank = 6 [6.16  $\pm$  0.46]; moderate sevoflurane rank = 5 [5.10  $\pm$  0.81]; deep sevoflurane rank = 6 [5.81  $\pm$  1.11];  $P < 0.0001$ ).

**Conclusions:** Whatever the molecular mechanism, anesthesia led to a massive reconfiguration of the repertoire of functional brain states that became predominantly shaped by brain anatomy (high function-structure similarity), giving rise to a well-defined cortical signature of anesthesia-induced loss of consciousness. (ANESTHESIOLOGY XXX; XXX:00-00)

ANESTHETICS are pharmacologic agents with a variety of neuronal and molecular targets. However, they share a common behavioral feature, *i.e.*, anesthesia-induced loss of consciousness. How can we characterize the common mechanism(s) of anesthesia-induced loss of consciousness beyond molecular pharmacology, *i.e.*, through an information-processing endpoint?<sup>1</sup> Several studies have demonstrated that intervoxel functional correlations in brain activity (sometimes called “functional connectivity”) change in parallel to arousal transition states such as sleep<sup>2</sup> or anesthesia.<sup>3,4</sup> Anesthetics disrupt frontoparietal long-range information processing and integration<sup>5,6</sup> in animals<sup>4</sup> and humans,<sup>7</sup> particularly with the posterior cingulate cortex,<sup>8</sup> and reduce thalamocortical functional correlation.<sup>9</sup> However, it is still unclear how anesthesia induces such functional disconnections.

### What We Already Know about This Topic

- Anesthesia-induced loss of consciousness is paralleled by a disruption of frontoparietal functional correlation, as measured by functional magnetic resonance imaging and electroencephalography. However, it is still unclear how anesthesia induces such a corticocortical disconnection.
- Dynamic-resting state is a recent analytical method to study large-scale brain networks, allowing the clustering of functional magnetic resonance images into functional brain states.

### What This Article Tells Us That Is New

- When moving from wakefulness to anesthesia, the anatomical structure of connections between brain areas becomes the main driver of the repertoire of functional states. Subjects given anesthesia lose the ability to generate flexible functional brain states that transcend brain anatomy.
- High similarity between brain structure and function is a new general signature of anesthesia-induced loss of consciousness.

Supplemental Digital Content is available for this article. Direct URL citations appear in the printed text and are available in both the HTML and PDF versions of this article. Links to the digital files are provided in the HTML text of this article on the Journal’s Web site ([www.anesthesiology.org](http://www.anesthesiology.org)). The work in this article has been presented as a poster presentation at the Euroanesthesia Meeting, May 28, 2016, London, United Kingdom, and as an oral presentation at the meeting of the French Society of Anesthesia and Critical Care, September 22, 2016, Paris, France. L.U., J.D.S., and A.J. contributed equally to this article.

From Commissariat à l’Énergie Atomique et aux Énergies Alternatives, Direction de la Recherche Fondamentale, NeuroSpin Center, Gif-sur-Yvette, France (L.U., A.J., J.T., P.B., M.D., S.D., B.J.); Cognitive Neuroimaging Unit, Institut National de la Santé et de la Recherche Médicale U992, Gif-sur-Yvette, France (L.U., A.J., J.T., P.B., M.D., S.D., B.J.); Department of Anesthesiology and Critical Care, Necker Hospital, University Paris Descartes, Paris, France (L.U.); Department of Anesthesiology and Critical Care, Sainte-Anne Hospital, University Paris Descartes, Paris, France (L.U.); Institut National de la Santé et de la Recherche Médicale U1127, Paris, France (J.D.S.); Physiological Investigations of Clinically Normal and Impaired Cognition Lab, Institut du Cerveau et de la Moelle épinière, Paris, France (J.D.S.); Collège de France, Paris, France (S.D.); Université Paris Sud, Université Paris-Saclay, Orsay, France (S.D.); Neurosurgery Department, Foch Hospital, Suresnes, France (B.J.); and the University of Versailles Saint-Quentin-en-Yvelines, Université Paris-Saclay, Versailles, France (B.J.).

Copyright © 2018, the American Society of Anesthesiologists, Inc. Wolters Kluwer Health, Inc. All Rights Reserved. Anesthesiology 2018; XXX:00-00

We previously demonstrated that during propofol anesthesia, resting-state brain activity dynamics loses its temporal diversity: during the loss of consciousness, the rich repertoire of brain states that exists in the awake state is suppressed, and the functional correlation matrix becomes rigidly parallel to the anatomical connectivity matrix.<sup>4</sup> Thus, dynamic resting-state study could provide a specific cortical signature of anesthesia-induced loss of consciousness. However, an alternative possibility is that the observed change was specific to the effect of propofol. Thus, it is important to extend the study of dynamic-resting state to other anesthetics, such as ketamine and sevoflurane.

While most anesthetics, including propofol, target  $\gamma$ -aminobutyric acid-mediated neurotransmission,<sup>10</sup> ketamine antagonizes *N*-methyl-D-aspartate receptors.<sup>11</sup> Sevoflurane is a  $\gamma$ -aminobutyric acid receptor type A agonist and *N*-methyl-D-aspartate antagonist<sup>12</sup> that induces a thalamocortical breakdown, while preserving the functional correlations between the thalamus and sensory cortices.<sup>13</sup>

One commonality between sevoflurane, propofol, and ketamine is the functional disconnection within frontoparietal networks,<sup>13,14</sup> suggesting a blockade of feedback connections.<sup>15</sup> This similarity between different anesthetic agents suggests a potential hypothesis for their common effect on consciousness: all may affect long-distance cortical networks, particularly the frontoparietal network thought to belong to a global neuronal workspace. The global neuronal workspace model is a theoretical model of conscious access that stipulates that information becomes conscious when it is available to a widely distributed prefrontoparietal and cingulate cortical network.<sup>16,17</sup> The global neuronal workspace is a theory of consciousness that has been introduced for the human brain. We recently demonstrated that the macaque brain is able to distinguish complex auditory sequences through a widely distributed brain network that we proposed as a “macaque global neuronal workspace” (Supplemental Digital Content, supplementary fig. 1, <http://links.lww.com/ALN/B756>) because of its homology to the human global neuronal workspace.<sup>18</sup> Moreover, we could demonstrate that this long-distance cortical network is disorganized during anesthesia.<sup>6</sup> Thus, anesthesia could be due to a specific shift in cortical dynamics, mainly within the global neuronal workspace nodes.

To test these hypotheses, we measured the dynamic resting-state activity of nonhuman primates during wakefulness and during different anesthetic agents and compared the matrix of functional correlations to the underlying anatomical (*i.e.*, structural) connectivity matrix. All anesthetics induced an identical endpoint, namely a resting-state repertoire devoid of dynamical diversity and dominated by a rigid brain configuration that is directly correlated to its underlying anatomical network. Thus, we could identify a common brain signature of anesthesia-induced loss of consciousness, independent from the specific type of anesthetic and molecular target.

## Materials and Methods

### Animals

Five rhesus macaques (*Macaca mulatta*), one male (monkey J) and four females (monkeys A, K, Ki, and R), 5 to 8 kg, 8 to 12 yr of age, were tested; three for each arousal state (awake: monkeys A, K, and J; propofol anesthesia: monkeys K, R, and J<sup>4</sup>; ketamine anesthesia: monkeys K, R, and Ki; sevoflurane anesthesia: monkeys Ki, R, and J). Note that nonhuman primate studies often only investigate a small number of animals. All procedures were conducted in accordance with the European Convention for the Protection of Vertebrate Animals used for Experimental and Other Scientific Purposes (Directive 2010/63/EU) and the National Institutes of Health's Guide for the Care and Use of Laboratory Animals. Animal studies were approved by the institutional Ethical Committee (Commissariat à l'Énergie atomique et aux Énergies alternatives; Fontenay aux Roses, France; protocols 10-003 and 12-086).

### Anesthesia Protocols

Monkeys received anesthesia either with ketamine,<sup>6</sup> propofol,<sup>4,6</sup> or sevoflurane. Levels of anesthesia were defined by the monkey sedation scale (based on spontaneous movements and the response to external stimuli presentation, shaking or prodding, toe pinch, and corneal reflex) with a clinical score determined at the beginning and the end of the scanning session and continuous electroencephalography monitoring.<sup>6</sup> During ketamine, deep propofol anesthesia, and deep sevoflurane anesthesia, monkeys stopped responding to all stimuli, reaching a state of general anesthesia. The monkeys (K, R, and Ki) that were scanned at a deep level of ketamine anesthesia<sup>6</sup> received an intramuscular injection of ketamine (20 mg/kg; Virbac, France) for induction of anesthesia, followed by a continuous intravenous infusion of ketamine (15 to 16 mg · kg<sup>-1</sup> · h<sup>-1</sup>) to maintain anesthesia. Atropine (0.02 mg/kg intramuscularly; Aguettant, France) was injected 10 min before induction, to reduce salivary and bronchial secretions.

For propofol anesthesia,<sup>4</sup> monkeys (K, R, and J) were scanned during moderate propofol sedation and deep propofol anesthesia (equivalent to general anesthesia). Monkeys were trained to be injected with an intravenous propofol bolus (5 to 7.5 mg/kg; Fresenius Kabi, France) to induce anesthesia. Induction was followed by target-controlled infusion (Alaris PK Syringe pump, CareFusion, USA) of propofol (moderate propofol sedation, 3.7 to 4.0  $\mu$ g/ml; deep propofol anesthesia, 5.6 to 7.2  $\mu$ g/ml) based on the “Paedfusor” pharmacokinetic model.<sup>19</sup> Although the “Paedfusor” model was mainly validated in humans, we previously applied this model to macaque monkeys with a high stability of both clinical scores and electroencephalography activity during the propofol anesthesia sessions.<sup>4,6</sup>

For sevoflurane anesthesia, monkeys (Ki, R, and J) were scanned during moderate and deep sevoflurane anesthesia. Monkeys received an intramuscular injection of ketamine (20 mg/kg; Virbac) for induction of anesthesia, followed by sevoflurane anesthesia (moderate sevoflurane anesthesia,

sevoflurane inspiratory/expiratory, 2.2/2.1 volume percent; deep sevoflurane anesthesia, sevoflurane inspiratory/expiratory, 4.4/4.0 volume percent; Abbott, France). We waited at least 80 min<sup>20</sup> before starting the scanning sessions during sevoflurane anesthesia to get a washout of the initial ketamine injection. To avoid artifacts related to potential movements throughout magnetic resonance imaging acquisition, a muscle-blocking agent was coadministered (cisatracurium, 0.15 mg/kg bolus intravenously, followed by continuous intravenous infusion at a rate of 0.18 mg · kg<sup>-1</sup> · h<sup>-1</sup>; GlaxoSmithKline, France) during the ketamine and moderate propofol sedation sessions.

For all the anesthesia experiments (ketamine, moderate and deep sevoflurane, moderate and deep propofol anesthesia), monkeys were intubated and ventilated as previously described.<sup>4</sup> Heart rate, noninvasive blood pressure (systolic/diastolic/mean), oxygen saturation, respiratory rate, end-tidal carbon dioxide, and cutaneous temperature were monitored (Maglife, Schiller, France) and recorded online (Schiller).

### Electroencephalography

To verify the anesthesia level during the ketamine, propofol, and sevoflurane sessions, we acquired scalp electroencephalography by using a magnetic resonance imaging-compatible system and custom-built caps, as previously described.<sup>4</sup> We performed an online analysis through visual assessment of electroencephalography traces. We interpreted the electroencephalography traces visually and defined the electroencephalography-based levels of anesthesia for the clinical sedative level<sup>6</sup> for ketamine, propofol, and sevoflurane anesthesia.

For ketamine, sedation levels were defined as follows<sup>6</sup>: level 1, awake state, posterior  $\alpha$  waves (eyes closed) and anterior  $\beta$  waves; level 2, light ketamine sedation, loss of alpha rhythm with a decrease of amplitude<sup>21</sup>; level 3, moderate ketamine sedation, persistent rhythmic  $\theta$  activity (4 to 6 Hz) with increasing amplitude and fast  $\beta$  activity (14 to 20 Hz) of low amplitude<sup>21</sup>; level 4, deep ketamine anesthesia, intermittent polymorphic  $\delta$  activity (0.5 to 2 Hz) of large amplitude, superimposed by a  $\beta$  activity (14 to 20 Hz) of low amplitude,<sup>21</sup> increase in  $\gamma$  power (30 to 100 Hz).<sup>22</sup> For propofol, sedation levels were defined as follows<sup>4,6</sup>: level 1, awake state, posterior  $\alpha$  waves (eyes closed) and anterior  $\beta$  waves; level 2, light propofol sedation, increase in the amplitude of  $\alpha$  waves and anterior diffusion of  $\alpha$  waves; level 3, moderate propofol sedation, diffuse and wide  $\alpha$  waves, and anterior theta waves<sup>23</sup>; level 4, deep propofol anesthesia (general anesthesia), diffuse delta waves, waves of low amplitude<sup>24</sup> and anterior  $\alpha$  waves (10 Hz)<sup>25</sup>; level 5, very deep sedation (deeper than level of general anesthesia), burst suppression. For sevoflurane, sedation levels were defined as follows: level 1, awake state, posterior  $\alpha$  waves (eyes closed) and anterior  $\beta$  waves; level 2, light sevoflurane sedation, increasing of frontal and central  $\beta$  waves<sup>26</sup>; level 3, moderate sevoflurane sedation, increased frontal delta,  $\alpha$  and  $\beta$

waves<sup>26</sup>; level 4, deep sevoflurane anesthesia (general anesthesia), diffuse delta waves and anterior  $\alpha$  waves<sup>26</sup>; level 5, very deep sedation (deeper than level of general anesthesia), burst suppression.

### Anatomical Data and Structural Connectivity

A detailed methodology was described in our previous study.<sup>4</sup> The anatomical (structural) data were derived from the CoCoMac2.0 database<sup>27</sup> of axonal tract tracing studies using regional map parcellation,<sup>28</sup> comprising 82 cortical regions of interest (41 regions of interest per hemisphere). Structural (*i.e.*, anatomical) connectivity data are expressed as matrices in which the 82 cortical regions of interest are displayed in x-axis and y-axis. Each cell of the matrix represents the strength of the anatomical connection between any pair of cortical areas. The CoCoMac connectivity matrix classifies the strength of the anatomical connections as weak, moderate, or strong, codified as 1, 2, and 3, respectively.<sup>4</sup>

### Functional Magnetic Resonance Imaging Data Acquisition

The data were collected between July 2011 and August 2016 (Supplemental Digital Content, supplementary tables 1–6, <http://links.lww.com/ALN/B756>). Monkeys were scanned on a 3-Tesla horizontal scanner (Siemens Tim Trio, Germany) with a single transmit-receiver surface coil customized to monkeys. Each functional scan consisted of gradient-echo planar whole-brain images (repetition time = 2,400 ms; echo time = 20 ms; 1.5-mm<sup>3</sup> voxel size; 500 brain volumes per run). Before each scanning session, a contrast agent, monocrystalline iron oxide nanoparticle (Feraheme, AMAG Pharmaceuticals, USA; 10 mg/kg, intravenous), was injected into the monkey's saphenous vein.<sup>4</sup> For the awake condition, monkeys were implanted with a magnetic resonance-compatible headpost and trained to sit in the sphinx position in a primate chair.<sup>18</sup> Monkeys sat inside the dark magnetic resonance imaging scanner without any task.<sup>4</sup> The eye position was monitored at 120 Hz (Iscan Inc., USA). For the anesthesia sessions, animals were positioned in a sphinx position, mechanically ventilated, and their physiologic parameters were monitored. In total, 157 runs were acquired: 31 awake runs (monkey A, 4 runs; monkey J, 18 runs; monkey K, 9 runs), 25 ketamine anesthesia runs (monkey K, 8 runs; monkey Ki, 7 runs; monkey R, 10 runs), 25 moderate sevoflurane sedation runs (monkey J, 5 runs; monkey Ki, 10 runs; monkey R, 10 runs), 20 deep sevoflurane anesthesia runs (monkey J, 2 runs; monkey Ki, 8 runs; monkey R, 11 runs), 25 moderate propofol sedation runs (monkey J, 2 runs; monkey K, 10 runs; monkey R, 12 runs), and 31 deep propofol anesthesia runs (monkey J, 9 runs; monkey K, 10 runs; monkey R, 12 runs) (Supplemental Digital Content, supplementary tables 1–6, <http://links.lww.com/ALN/B756>). To compare the propofol, ketamine, and sevoflurane anesthesia states (Supplemental Digital Content, supplementary fig. 2, <http://links.lww.com/ALN/B756>), we included the propofol anesthesia data from a previous experiment.<sup>4</sup>

### Functional Magnetic Resonance Imaging Preprocessing

Functional images were reoriented, realigned, and rigidly coregistered to the anatomical template of the monkey Montreal Neurologic Institute (Montreal, Canada) space with use of Python programming language and Oxford Centre Functional Magnetic Resonance Imaging of the Brain Software Library software (United Kingdom, <http://www.fmrib.ox.ac.uk/fsl/>; accessed February 4, 2018).<sup>18</sup> In total, 157 functional magnetic resonance imaging runs were analyzed for the experiment (31 runs for the awake state, 25 runs for ketamine anesthesia, 25 runs for moderate propofol sedation, 31 runs for deep propofol anesthesia, 25 runs for moderate sevoflurane sedation, and 20 runs for deep sevoflurane anesthesia). Global signal from the images was regressed out to remove any confounding effect due to physiologic changes (e.g., respiratory or cardiac changes) associated with ketamine, sevoflurane, or propofol anesthesia. Voxel time series were filtered with low-pass (0.05-Hz cutoff) and high-pass (0.0025-Hz cutoff) filters and a zero-phase fast-Fourier notch filter (0.03 Hz) to remove an artifactual pure frequency present in all the data.<sup>4</sup> The variance of each time series was normalized; thus, covariance matrices correspond to correlation matrices.<sup>29</sup>

### Functional Magnetic Resonance Imaging Resting-state Analysis

A detailed methodology of the analysis of the resting-state functional magnetic resonance imaging was described in our previous study.<sup>4</sup> Resting-state functional magnetic resonance imaging data are expressed as matrices in which the 82 cortical regions of interest are displayed on the x-axis and y-axis. Each cell of the matrix represents the intensity of the “functional” correlation between any pair of cortical areas. We applied two different approaches to analyze resting-state functional magnetic resonance imaging: (1) stationary resting-state functional magnetic resonance imaging connectivity, which is the classical method to compute intercortical “functional” correlation within the resting-state data; (2) dynamical resting-state functional magnetic resonance imaging connectivity, which is a recently described method that can cluster the functional magnetic resonance imaging dataset into several “brain states,” *i.e.*, “functional configurations” of the brain, that build up the stationary resting state.<sup>4,29</sup> These “brain states” can be similar (high correlation between the structural and the functional matrices) or dissimilar (low correlation between the structural and the functional matrices) to the underlying brain structure. Stationary and sliding window zero-lag covariance matrices were estimated for each arousal or anesthetic condition and session.<sup>29</sup>

**Stationary Connectivity Analysis.** Stationary connectivity analysis refers to the classical approach for resting-state functional magnetic resonance imaging analysis during which we measured the intervoxel correlation (also called “functional connectivity”) between different brain areas (regions of interest) and expressed it as a graphical matrix where colors

express the strength of correlation between pairs of regions of interest. The graphical matrix displays the whole cortical map of interregions of interest correlations.

As previously described,<sup>4</sup> we first estimated for each arousal or anesthetic condition, *c*, and functional magnetic resonance imaging session, *s*, the covariance matrix  $C_{c,s}$  to confirm the presence of long-range stationary cortical connections whatever the arousal or anesthetic condition. To estimate  $C_{c,s}$  for each region of interest, a time series was extracted for each session, averaging all voxels within a region of interest at a given brain volume. The matrix entry  $C_{c,s}(i,j)$  indicates the temporal correlation of the average functional magnetic resonance imaging signal extracted from regions of interest *i* and *j* (for example, *i* = 27 for left posterior cingulate cortex and *j* = 41 for left dorsolateral premotor cortex; Supplemental Digital Content, supplementary table 7, <http://links.lww.com/ALN/B756>). We estimated covariance from the regularized precision matrix, applied the graphical Least Absolute Shrinkage and Selection Operator method, and placed a penalty on the L1 norm of this precision matrix to promote sparsity. Thus, we could generate a connectivity matrix (82 × 82) per each arousal or anesthetic condition. We then applied Fisher transform using the formula  $z = ar \tanh(c)$  and could generate a covariance matrix  $Z_{c,s}$  for each arousal or anesthetic condition and session (fig. 1; Supplemental Digital Content, supplementary figs. 3 and 4, <http://links.lww.com/ALN/B756>). By averaging  $Z_{c,s}$  matrices across functional magnetic resonance imaging sessions, we obtained an average matrix  $Z_c$  for each arousal or anesthetic condition (fig. 1A). For propofol conditions, average  $Z_c$  matrices were reported in our previous study.<sup>4</sup> To estimate the balance between positive and negative correlations between cortical regions of interest, we calculated for each arousal or anesthetic condition and session the average of positive *z* values of  $Z_{c,s}$  and also the rate between negative and positive *z* values.

**Dynamical Connectivity Analysis.** Dynamical connectivity analysis refers to a recently described method that aims at better characterizing the underlying brain dynamics during the scan session instead of averaging these data over the scan session as with stationary resting-state analysis. In fact, whereas stationary connectivity estimates functional correlations between cortical regions during the whole functional magnetic resonance imaging acquisition session (computing one average graphical matrix for the whole session), the dynamical connectivity approach takes into account the fluctuations of the functional correlations that occur during the functional magnetic resonance imaging session (computing one graphical matrix every 84 s of the 20-min session, which corresponds to the so-called sliding window method, as previously described<sup>4</sup>). With data-mining approaches (k-means algorithm in our case), the functional magnetic resonance imaging dataset of the session is split into several clusters that are called “brain states” and that correspond to “functional configurations” of the brain.<sup>4,29</sup> These “brain states” can express high or low similarity with the anatomical connectivity.

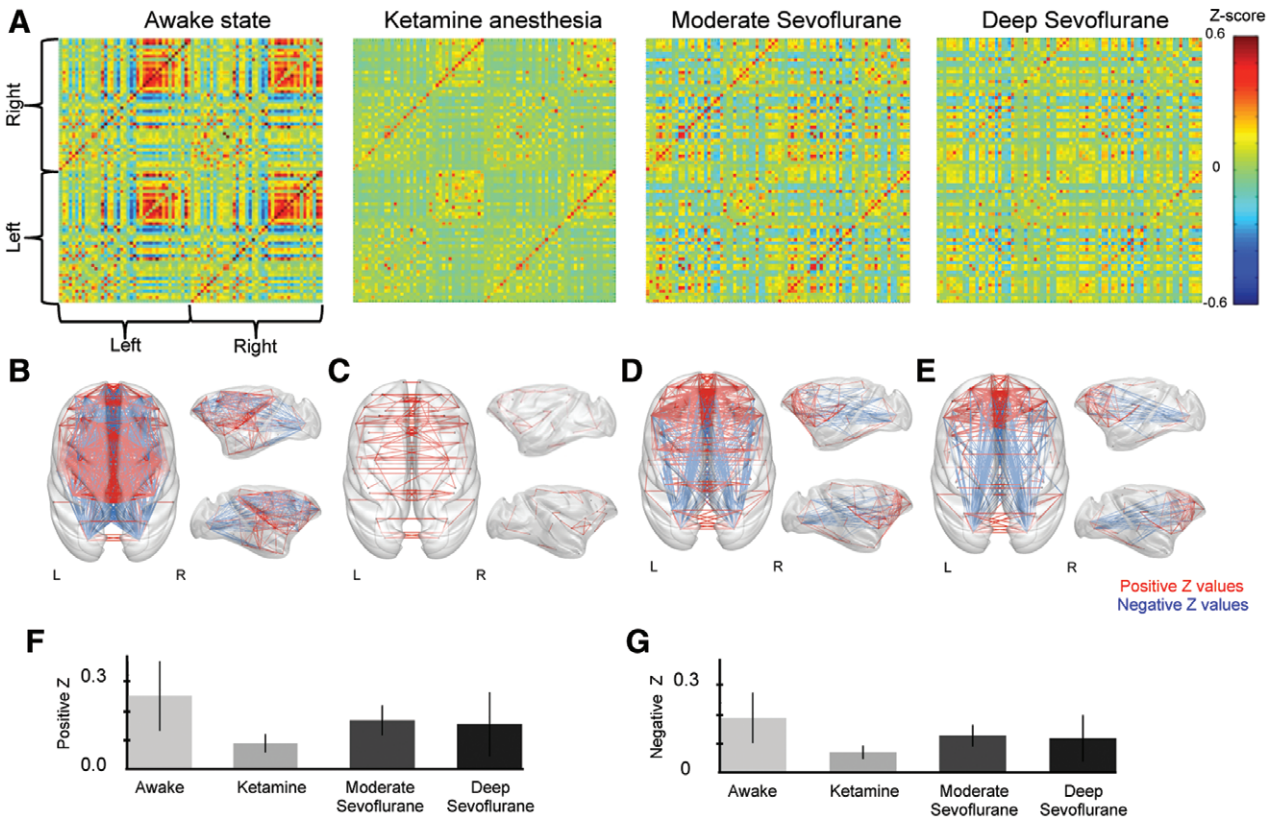


**Fig. 1.** Anesthesia effects on stationary intervoxel correlations in the cortex. (A) Average correlation matrices showing the presence of stationary correlations for the awake state, ketamine anesthesia, and sevoflurane anesthesia. (B–E) All significant correlations are plotted into glass brains that display absolute functional correlation strength higher than 0.2 for the awake state (B; Student’s *t* tests, with the null hypothesis of zero correlation,  $P < 0.01$ , false discovery rate corrected), ketamine anesthesia (C), moderate sevoflurane sedation (D), and deep sevoflurane anesthesia (E); red lines represent positive correlations between regions of interest; blue lines represent negative correlations. (F) Average positive z values within the awake state, ketamine, and sevoflurane anesthesia. In all plots, error bars represent SD. (G) Average negative z values within the awake state, ketamine, and sevoflurane anesthesia. In all plots, error bars represent SD. L = left; R = right.

We estimated sliding window Fisher-transformed covariance matrices  $Z_{c,s,w}$  for each arousal condition (c), session (s), and time window (w).<sup>30</sup> Covariance matrices from windowed segments of the time series were computed with a Hamming window (width = 84s, which corresponds to 35 scans of 2,400 ms each), sliding with steps of one scan, resulting in 464 windows per session. For each condition and session, we produced a three-dimensional matrix,  $C_{c,s,w}$  sized  $82 \times 82 \times 464$ , which was Fisher transformed ( $Z_{c,s,w}$ ) before further analysis.

We determined the dominant recurrent patterns of brain correlations (brain states) by means of an unsupervised clustering method along the time dimension of the  $Z_{c,s,w}$  matrix.<sup>29</sup> To evaluate the structure of reoccurring correlation patterns, we applied the k-means clustering algorithm<sup>31</sup> to  $Z_{c,s,w}$  matrices, using the L1 distance function (Manhattan distance), as implemented in Matlab (MathWorks, USA). This analysis was performed on the data from different arousal conditions (awake state + ketamine anesthesia (fig. 2); awake state + moderate sevoflurane sedation + deep sevoflurane anesthesia (fig. 3), awake state + ketamine anesthesia + moderate

sevoflurane sedation + deep sevoflurane anesthesia + moderate propofol sedation + deep propofol anesthesia (Supplemental Digital Content, supplementary figs. 5, A and B; 6; 7–10, <http://links.lww.com/ALN/B756>); ketamine anesthesia + moderate sevoflurane sedation + deep sevoflurane anesthesia + moderate propofol sedation + deep propofol anesthesia (Supplemental Digital Content, supplementary figs. 5C and 5D, <http://links.lww.com/ALN/B756>), mixed to avoid any bias.

Covariance values between all regions of interest were included ( $[82 \times (82 - 1)] / 2 = 3,321$  features per matrix).  $Z_{c,s,w}$  matrices were subsampled along the time dimension before clustering. The resulting centroids or median clusters (brain state [n] with  $n = 1$  to 7; each brain state is sized  $82 \times 82$ ) were then used to initialize a clustering of all data, obtaining a matrix of brain states  $B_{c,s,w}$  which, for a given arousal condition and session, is a vector of length 464, valued 1 to 7, because each matrix in  $Z_{s,p,w}$  is assigned a brain state. The number of brain states was determined following protocols found in Bartfeld *et al.* and Allen *et al.*,<sup>4,29</sup> with a predefined number of brain states (n), 1 to 7. The method

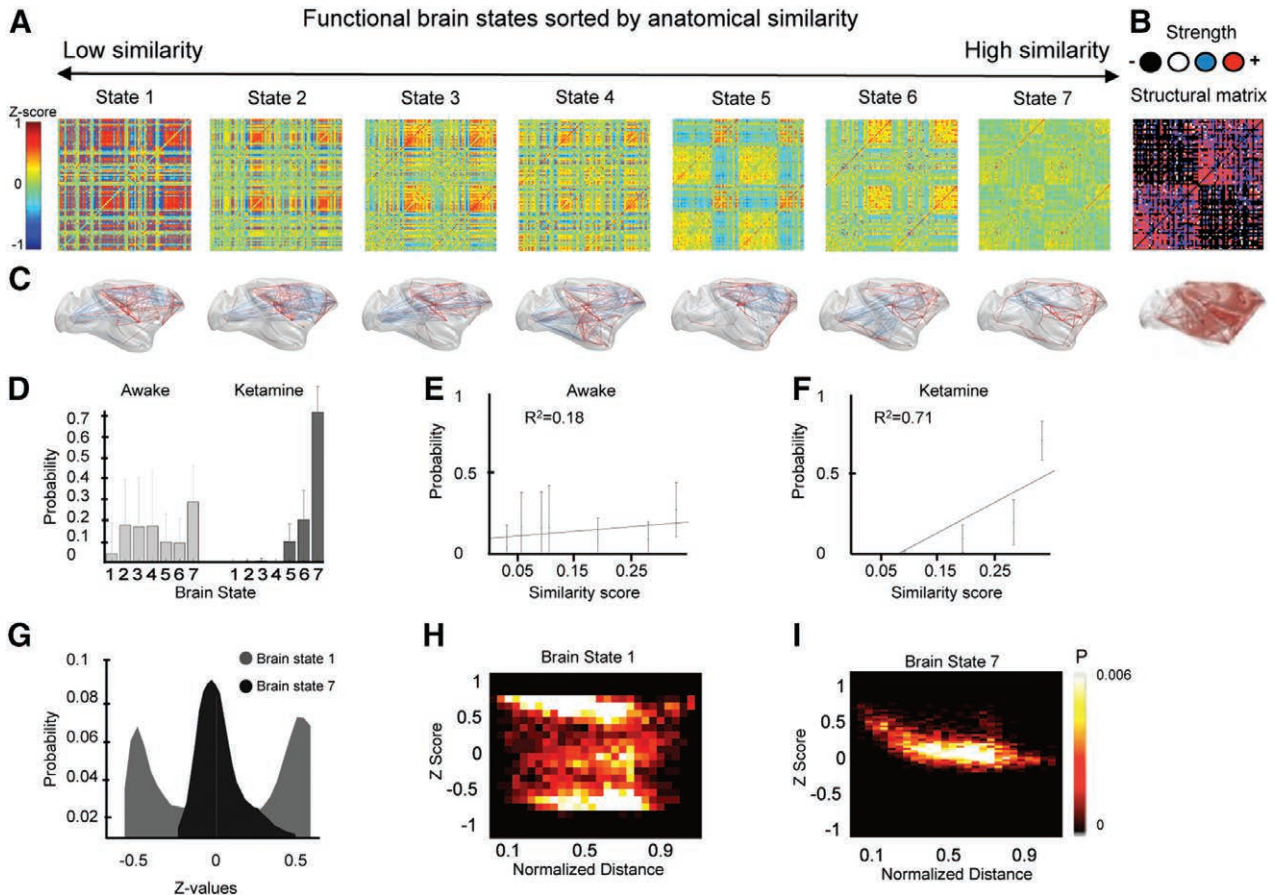


**Fig. 2.** Ketamine effects on cortical dynamical correlations. (A) Seven brain states, obtained by unsupervised clustering of the  $Z_{c,s,w}$  matrix (awake state + ketamine anesthesia). Brain states are sorted according to their similarity to the structural connectivity matrix. (B) Structural connectivity matrix derived from the CoCoMac atlas of anatomical macaque cortical connectivity. Colors represent the four grades of connectivity intensity (*black* = 0; *white* = 1; *blue* = 2; and *red* = 3). (C) Brain renders displaying the 400 strongest links for each brain state; *red lines* represent positive correlations between regions of interest; *blue lines* represent negative correlations. (D) Probability distributions of brain states for the awake state and ketamine anesthesia. Each bar represents the within-condition probability of occurrence of a state. *Error bars* stand for SD. (E–F) Probability of occurrence of each brain state as a function of the similarity between functional correlation and structural connectivity for the awake state (E) and ketamine anesthesia (F). (G) Normalized probability distribution of all z values for brain states 1 (the least similar to structure) and 7 (the most similar to structure). (H and I) Two-dimensional normalized histograms for brain state 1 (H) and brain state 7 (I) z values, as a function of distance between pairs of regions of interest.

gives for each point in time the most likely state of functional correlations. This enables comparison of how these states and their dynamics change with the level of arousal or the anesthetic agent that was administered to the animal.

To explore the dependence of brain dynamics and arousal condition, a measure of similarity between anatomical connectivity (CoCoMac2.0) and functional correlation was defined, to class all brain states along this dimension.<sup>4</sup> The similarity score was computed from the correlation coefficient between the vectorized structural matrix and each vectorized brain state from the clustering analysis. All brain states were ordered in ascending order of similarity to the structure with the similarity score. To quantify the relation between the probability of occurrence of a brain state and the similarity score, a regression analysis was done for each arousal condition to quantify the  $\beta$  value, the  $R^2$ , and a  $P$  value. The

$\beta$  value measured the strength of the function-structure similarity score effect on the functional repertoire of the brain states. The distance between regions of interest was calculated as the L2 norm in the three-dimensional space, by use of the Montreal Neurologic Institute coordinates of CoCoMac as input. We also calculated the duration of each brain state (the average length of sequences of a given brain state in the  $B_{c,s,w}$  matrix; Supplemental Digital Content, supplementary fig. 2, <http://links.lww.com/ALN/B756>).

#### Connectivity within the Global Neuronal Workspace Nodes.

As mentioned in the introduction, the global neuronal workspace theory of consciousness states that information becomes conscious when it is available to a widely distributed cortical network that includes prefrontal, parietal, and cingulate cortices.<sup>16,17</sup> Because anesthesia has been reported to disorganize this long-distance cortical network during auditory

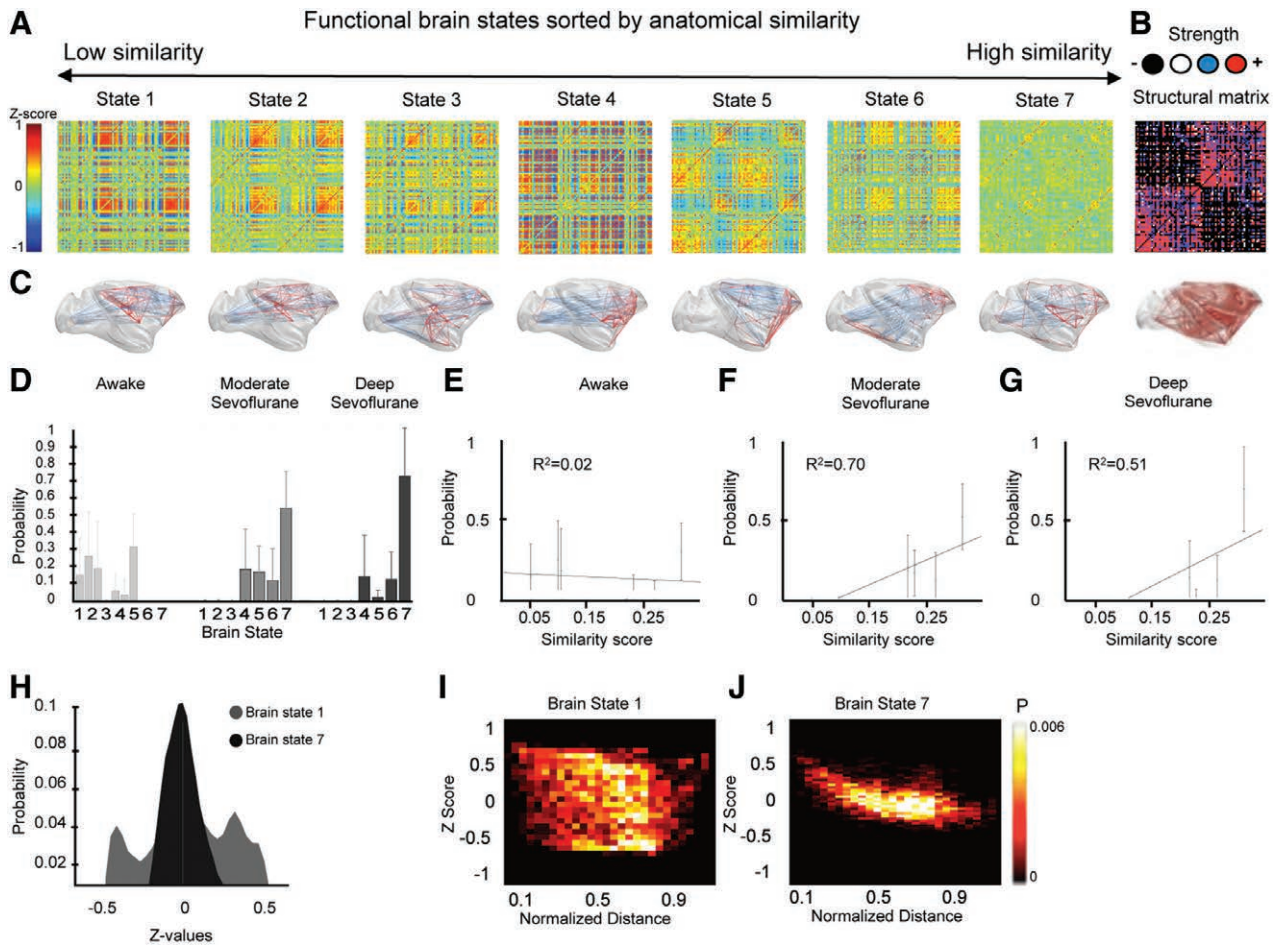


**Fig. 3.** Sevoflurane effects on cortical dynamical correlations. (A) Seven brain states, obtained by unsupervised clustering of the  $Z_{c,s,w}$  matrix (awake state + moderate sevoflurane sedation + deep sevoflurane anesthesia). (B) Structural connectivity matrix derived from the CoCoMac atlas of anatomical macaque cortical connectivity. Colors represents the four grades of connection intensity (black = 0; white = 1; blue = 2; and red = 3). (C) Brain renders displaying the 400 strongest links for each brain state. Red lines represent positive connections between regions of interest; blue lines represent negative connections. (D) Probability distributions of brain states for the awake state and sevoflurane anesthesia (moderate and deep). Each bar represents the within-condition probability of occurrence of a state. Error bars stand for SD. (E–G) Probability of occurrence of each brain state as a function of the similarity between functional and structural connectivity for the awake state (E), moderate sevoflurane sedation (F), and deep sevoflurane anesthesia (G). (H) Normalized probability distribution of all z values for brain states 1 (the least similar to structure brain state) and 7 (the most similar to structure brain state). (I and J) Two-dimensional normalized histograms for brain state 1 (I) and brain state 7 (J) z values, as a function of distance between pairs of regions of interest.

tasks,<sup>6</sup> we explored the effect of anesthesia on intervoxel correlation (functional connectivity) within the global neuronal workspace nodes and between sensorimotor areas and global neuronal workspace nodes during resting state.

**Statistical Analyses**

This study was performed in a small sample size. Thus, no “a priori” power calculation was conducted.

**Stationary Connectivity Analysis.** To test for statistical significance of connectivity between brain regions (cortical regions of interest) in different arousal and anesthetic conditions, Student’s *t* tests were performed with the null hypothesis of zero correlation. To correct for the multiple comparisons, the false discovery rate method was used, with a *P* value of 0.0001. All significant connections with an

absolute connectivity strength higher than 0.3 were plotted into glass brains.

To test for statistical differences between arousal and anesthetic conditions in terms of positive and negative correlations, we applied a bootstrapping method<sup>32</sup> with Matlab R2014a software. The bootstrapping technique allows the estimation of the sampling distribution by a random-sampling method (bootstrap analysis). In our study we obtained for every arousal and anesthetic condition and session the mean value of all positive connections of every region of interest as follows:

$$Z_{c,positive} = \sum_{i=1}^N \frac{Z_{pos,c,s}(i,j) \text{ if } i \neq j}{N}$$

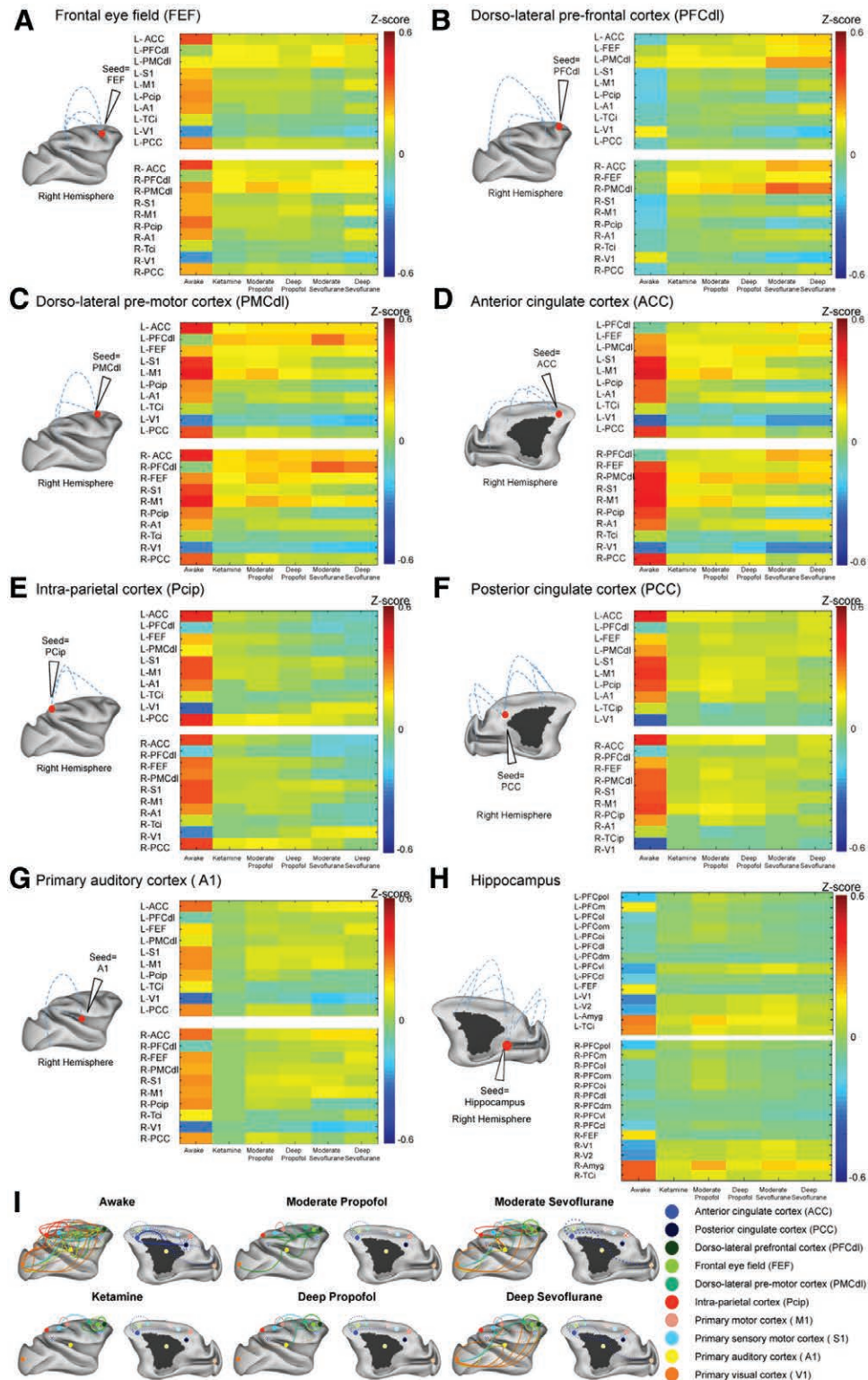


**Fig. 4.** Anesthesia effects on stationary intervoxel correlations within the macaque global neuronal workspace. Average correlation matrices for the awake state and anesthesia (ketamine anesthesia, moderate propofol sedation, deep propofol anesthesia, moderate sevoflurane sedation, and deep sevoflurane anesthesia; Student's *t* tests, with the null hypothesis of zero correlation,  $P < 0.001$ , false discovery rate corrected). On the *x*-axis, arousal states. On the *y*-axis, regions from the macaque global neuronal workspace as defined in Uhrig *et al.*<sup>18</sup> (ACC, PFCpol, FEF, PMCDl, S1, M1, Pcip, A1, TCi, V1, PCC of the left [L] and right [R] hemisphere). For each region (FEF [A], PFCdl [B]...), the matrix represents the functional correlation between the defined region (seed) and the remaining global neuronal workspace regions. Anesthesia decreases the functional correlation between the global neuronal workspace (Continued)

**Fig. 4.** (Continued), and its remaining areas such as FEF (A), PMCdl (C), ACC (D), Pcip (E), PCC (F), and A1 (G). However, anesthesia increases the functional correlation within prefrontal areas such as PFCdl (B). (I) Schematic representation of cerebral correlations of the macaque global neuronal workspace (ACC, PCC, PFCdl, FEF, PMCdl, Pcip, M1, S1, V1, A1; absolute correlation strength higher than 0.3) of the right hemisphere for the awake state and all anesthetic states. The results of the interregion ANOVA comparisons are displayed as *P* value matrices in Supplemental Digital Content, supplementary fig. 11, <http://links.lww.com/ALN/B756>. A1 = primary auditory cortex; ACC = anterior cingulate cortex; Amyg = amygdala; FEF = frontal eye fields; M1 = primary motor cortex; PCC = posterior cingulate cortex; PFCcl = centrolateral prefrontal cortex; PFCdl = dorsolateral prefrontal cortex; PFCdm = dorsomedial prefrontal cortex; PFCm = medial prefrontal cortex; PFCol = prefrontal polar cortex; PFCom = orbitomedial prefrontal cortex; PFCoi = orbitoinferior prefrontal cortex; PFCpol = prefrontal polar cortex; PFCvl = ventrolateral prefrontal cortex; PMCdl = dorsolateral premotor cortex; Pcip = intraparietal cortex; S1 = primary somatosensory cortex; TCi = inferior temporal; V1 = visual area 1; V2 = visual area 2.

Where  $Z_{pos}$  represents all *z* values that are positive in a matrix  $Z_{c,s}$ , and *N* is the total number of positive *Z* values. Then we subtracted the mean value of two conditions (for example,  $Z_{awake, positive} - Z_{ketamine, positive}$ ) and called it the observed difference between conditions. We calculated the null distribution of  $Z_{c, positive}$  value differences between conditions, shuffling scanning sessions across conditions (thus breaking any possible dependence between arousal/anesthetic condition and connectivity value) and repeated the subtraction analysis 100,000 times, obtaining a distribution of random mean *Z* value differences that approaches a Gaussian distribution. This distribution is called null distribution and is the distribution of expected differences under the hypothesis of no relation between sedation condition and mean positive connectivity. If our observed difference in  $Z_{c, positive}$  is truly reflecting a difference between sedation conditions, its value should be located on a tail of the null distribution. We fitted a Gaussian to the null distribution to obtain a normalized  $Z_{c, positive}$  by subtracting from the observed  $Z_{condition}$  the mean value of the fitted Gaussian and dividing it by the SD of the Gaussian distribution. We obtained the *P* value corresponding to the normalized  $Z_{c, positive}$  as the cumulative probability of the normalized observed difference in the normalized Gaussian distribution. This procedure was used each time a bootstrap analysis was performed in the analysis.

We also calculated for each condition and each session the rate of negative to positive *Z* values (Supplemental Digital Content, supplementary fig. 3, <http://links.lww.com/ALN/B756>), to quantify changes in negative *z* values across conditions, as

$$rate_{c,s} = \frac{\sum_{i=1}^N \sum_{j=1}^N (abs(Z_{i,j}) | Z_{i,j} < 0)}{\sum_{i=1}^N \sum_{j=1}^N Z_{i,j} | Z_{i,j} > 0}$$

**Dynamical Connectivity Analysis.** The differences in brain state composition across arousal states was evaluated through a mixed-effects one-way ANOVA (R software v3.4.3, <http://www.r-project.org>; accessed February 4, 2018), with mean rank, that is, the result of averaging each brain state time series, valued from 1 to 7, as dependent variable, the vigilance condition as independent variable, and the animal identity as random variable. Similarly, a mixed-effects ANOVA (R software v3.4.3) was run to quantify the effect of sedation on the probability of brain

state 7. The normalized probability distribution of *z* values for brain states 1 and 7, binning correlation values in 45 bins, is represented in figure 2G and figure 3H. Two-dimensional normalized histograms of the same brain states *z* values, as a function of distance between pairs of regions of interest, are represented in figure 2, H and I, and figure 3, I and J.

**Connectivity within the Global Neuronal Workspace Nodes.**

To explore the intervoxel correlation (functional connectivity) within the global neuronal workspace nodes, we extracted the values from the whole-brain matrices and applied a one-way ANOVA. The *P* values are displayed in interregions matrices within the global neuronal workspace nodes and sensorimotor areas (Supplemental Digital Content, supplementary figs. 11 and 12, <http://links.lww.com/ALN/B756>). The plan of this statistical analyses section evolved after examination of the data and in response to peer reviewer suggestions.

**Results**

**Animal Model**

Physiologic parameters related to hemodynamic, ventilation, and temperature were kept constant during each experiment (Supplemental Digital Content, supplementary table 8, <http://links.lww.com/ALN/B756>). In all sessions and in all animals, the moderate anesthesia level for propofol and sevoflurane corresponded to level 3, as defined by the monkey sedation scale and electroencephalography traces (Supplemental Digital Content, supplementary table 9, <http://links.lww.com/ALN/B756>), and the deep anesthesia level for ketamine, propofol, and sevoflurane corresponded to level 4, as defined by the monkey sedation scale and electroencephalography traces (Supplemental Digital Content, supplementary table 10, <http://links.lww.com/ALN/B756>).

**Stationary Connectivity Results**

By averaging the functional correlations between cortical regions over each resting-state functional magnetic resonance imaging scan session time, we obtained stationary matrices of functional correlations (also called “functional connectivity”) in the awake state and with different anesthetics. (figs. 1 and 4; Supplemental Digital Content, supplementary figs. 3, 4, 11, 13, <http://links.lww.com/ALN/B756>). This stationary connectivity analysis confirmed the persistence of some

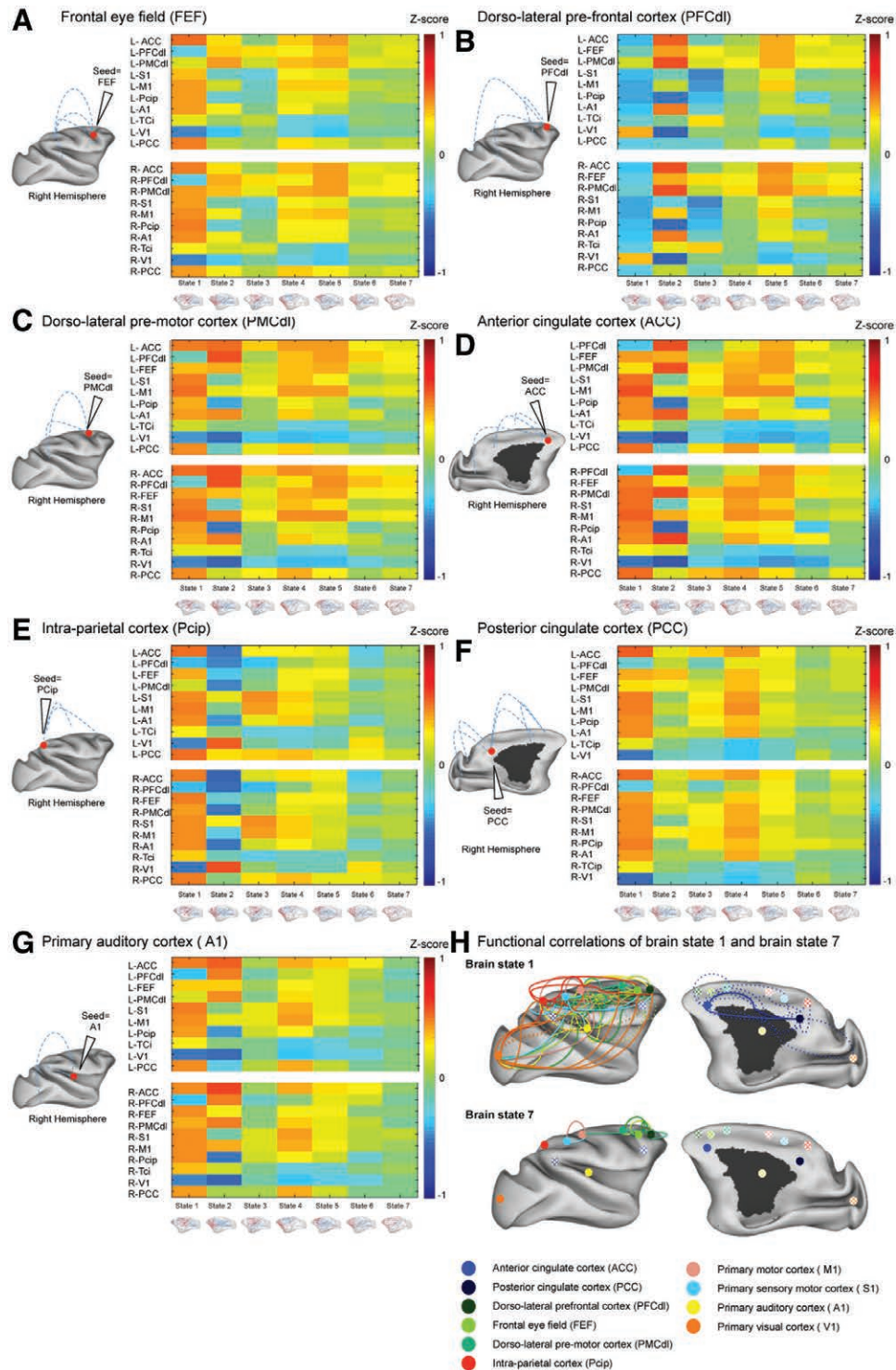


**Fig. 5.** Anesthesia effects on dynamical correlations within the macaque global neuronal workspace. The seven brain states, obtained by unsupervised clustering of the  $Z_{c,s,w}$  matrix and brain states are sorted according to their similarity to the structural connectivity matrix (awake state + ketamine anesthesia + moderate propofol sedation + deep propofol anesthesia + moderate sevoflurane sedation + deep sevoflurane anesthesia). Average correlation matrices for every brain state, ordered from 1 to 7. On the x-axis, brain state 1 to 7. On the y-axis, studied regions of interest of the macaque global neuronal workspace (ACC, PFCpol, FEF, PMCDl, S1, M1, Pcip, A1, TCi, V1, PCC of the left [L] and right [R] hemisphere) connected to the seed. Changes of functional correlation across the 7 brain states between the global neuronal workspace and its remaining areas such as FEF (A), PFCdl (B), PMCDl (C), ACC (D), Pcip (E), PCC (F), and A1 (G). Remarkably, the predominant anesthesia state (state 7) is characterized by a very low functional correlation within the global neuronal workspace; while (Continued)

**Fig. 5.** (Continued). the predominant wakefulness state (state 1) shows a high functional correlation within the global neuronal workspace. (H) Schematic representation of the macaque global neuronal workspace correlations (absolute correlation strength higher than 0.2) of the right hemisphere for brain state 1 and brain state 7. *Hatched areas* correspond to nodes that are on the other side of the hemisphere, thus displayed by transparency. The results of the interregion ANOVA comparisons are displayed as *P* value matrices in Supplemental Digital Content, supplementary fig. 12, <http://links.lww.com/ALN/B756>. A1 = primary auditory cortex; ACC = anterior cingulate cortex; FEF = frontal eye fields; M1 = primary motor cortex; PCC = posterior cingulate cortex; Pcip = intraparietal cortex; PFCdl = dorsolateral prefrontal cortex; PFCpol = prefrontal polar cortex; PMCdl = dorsolateral premotor cortex; S1 = primary somatosensory cortex; TCi = inferior temporal; V1 = visual area 1.

long-range connections during anesthesia<sup>4,33</sup> (fig. 1A–E), although many cortical areas displayed a decrease in inter-voxel correlations during anesthesia (Supplemental Digital Content, supplementary fig. 13, <http://links.lww.com/ALN/B756>).

#### Stationary Functional Correlations in the Awake State.

In the awake state, positive correlations formed a complex long-distance network comprising anterior and posterior cingulate cortex, dorsomedial prefrontal cortex, as well as primary motor, sensorimotor, visual, and auditory cortices (fig. 4A–I, Supplemental Digital Content, supplementary fig. 4, A and C, <http://links.lww.com/ALN/B756>). In the awake state, a large number of negative correlations were also present (fig. 1, fig. 4A–H; Supplemental Digital Content, supplementary fig. 4, A and C, <http://links.lww.com/ALN/B756>).

#### Stationary Functional Correlations during Anesthesia.

Under ketamine anesthesia, we mainly observed a persistence of positive correlations (fig. 1C, fig. 4A–F), but the average positive *z* value was reduced compared to the awake state (fig. 1F; bootstrap analysis, awake *vs.* ketamine anesthesia,  $P < 0.0001$ ). As previously reported for propofol,<sup>4</sup> the ratio of negative to positive correlations also diminished significantly during ketamine anesthesia compared to the awake state (Supplemental Digital Content, supplementary fig. 3C, <http://links.lww.com/ALN/B756>; bootstrap analysis, awake *vs.* ketamine anesthesia,  $P < 0.0001$ ).

During sevoflurane anesthesia, positive and negative correlations persisted (fig. 1D–E, fig. 4A–H), but the average positive *z* value was again reduced compared to the awake state (fig. 1F; bootstrap analysis, awake *vs.* moderate sevoflurane sedation,  $P < 2 \times 10^{-3}$ ; awake *vs.* deep sevoflurane anesthesia,  $P < 4 \times 10^{-3}$ ; moderate sevoflurane sedation *vs.* deep sevoflurane anesthesia,  $P = 0.29$ ). No significant differences between the ratio of negative to positive correlations with sevoflurane anesthesia compared to the awake state were found (Supplemental Digital Content, supplementary fig. 3C, <http://links.lww.com/ALN/B756>; bootstrap analysis, awake *vs.* moderate sevoflurane sedation,  $P = 0.26$ ; awake *vs.* deep sevoflurane anesthesia,  $P = 0.40$ ; moderate sevoflurane anesthesia *vs.* deep sevoflurane anesthesia,  $P = 0.59$ ). These results suggest that during both ketamine anesthesia and sevoflurane anesthesia, the average coupling between brain regions is weaker than in the awake state (fig. 4, Supplemental Digital Content, supplementary fig. 4, <http://links.lww.com/ALN/B756>). These results are in line with our previous findings during propofol anesthesia.<sup>4</sup>

#### Stationary Functional Correlations within the Macaque Global Neuronal Workspace.

To study the specific effect of anesthetics on the global neuronal workspace, we examined the functional correlation within the key nodes of the macaque global neuronal workspace as previously characterized<sup>18</sup> (fig. 4). All anesthetics (ketamine, sevoflurane, propofol) strikingly disconnected the posterior cingulate cortex and parietal cortex from the remaining bilateral global neuronal workspace nodes (fig. 4, E and F), in line with our previous finding.<sup>6</sup> Anesthesia disconnected frontal eye fields and premotor areas from parietal and cingular cortices, while preserving and sometimes even increasing intrafrontal functional correlations (fig. 4C). It should be noted that anesthesia decreased functional correlation between hippocampus and amygdala/temporal cortex (fig. 4H). As summarized in fig. 4I, functional correlations were strongly decreased within the global neuronal workspace with anesthesia with a striking suppression of posterior cingulate functional correlations with the remaining global neuronal workspace, whatever the anesthetic. Such “static” (or stationary) results, however, obtained by averaging functional magnetic resonance imaging data over the whole-time scan period, may mask larger changes in cortical dynamics during the same scan session. In the next step, we therefore compared the dynamics of resting-state functional magnetic resonance imaging networks in macaque monkeys in the awake state and during ketamine and sevoflurane anesthesia.

#### Dynamical Connectivity Results with Ketamine Anesthesia

We extracted from the dynamics of functional correlation seven representative “brain states” matrices using k-means data-mining algorithm (see Materials and Methods section; figs. 2 and 5; Supplemental Digital Content, supplementary figs. 2, 5, 6, <http://links.lww.com/ALN/B756>). These brain states (fig. 2, A and C) were ranked according to their similarity to the brain anatomy (CoCoMac structural connectivity matrix<sup>27</sup>; fig. 2B), to probe the hypothesis that the dynamic long-range functional correlation matrix reduces to the underlying structural anatomical connectivity matrix (fig. 2B) during ketamine anesthesia.

The probability of occurrence of each of the seven brain states varied with the arousal condition. In the awake condition, most brain states (except brain state 6) had a similar probability of occurrence, and this probability was not modulated by the similarity of the functional correlation to the structural connectivity ( $\beta$  value = 0.29;  $R^2 = 0.18$ ;  $P = 0.34$ ; fig. 2, D and E). During ketamine anesthesia, the probability distribution of the brain states was modified (fig. 2, D and F). Brain

states 1, 2, and 3 (with the lowest similarity to the anatomical structure) never occurred during ketamine anesthesia. The more similar a brain state was to the anatomical connectivity, the more probable it became during ketamine anesthesia ( $\beta$  value = 1.92;  $R^2 = 0.71$ ;  $P = 0.016$ ). The distribution of brain states relative to the anatomical connectivity matrix was significantly altered by ketamine anesthesia (ANOVA mean rank expressed as rounded rank: awake = 4 [mean, 4.49 ± 0.88]; ketamine anesthesia = 7 [mean, 6.60 ± 0.16];  $F_{(1,50)} = 41.26$ ,  $P < 0.0001$ ). The occurrence probability of some brain states, (notably states 1, 2, and 3) those with the lowest similarity to anatomy, was so low that they never occurred during ketamine anesthesia. Brain state 7, most similar to anatomical structure, became functionally dominant (ANOVA state 7 probability; awake = 0.28 [SD, 0.17]; ketamine = 0.71 [SD, 0.12];  $F_{(1,50)} = 52.77$ ,  $P < 0.0001$ ; fig. 2D).

The larger the similarity score to the anatomical connectivity, the more probable a brain state was during anesthesia, and the weaker the functional coupling between brain regions (brain state 7; fig. 5A–H; Supplemental Digital Content, supplementary fig. 6, <http://links.lww.com/ALN/B756>). The SD of the distribution of functional correlation values increased as the similarity score decreased ( $\beta$  value = -3.20;  $R^2 = 0.87$ ,  $P = 0.002$ ). The change in SD became obvious when comparing the histogram of functional correlation measures for brain states 7 and 1 (fig. 2G).

The cortical functional correlations changed with the spatial distance between brain regions in all brain states. For brain state 1, functional correlation strength diminished only moderately with distance, and dense strong positive and negative connections were detected even for very distal pairs of nodes (fig. 2H). In contrast, brain state 7 (fig. 2I) had a predominance of short-range connections, and functional correlations dropped to zero as distance increased. Statistical analysis showed a monotonic decrement in correlation strength as a function of distance along the similarity axis: while  $z$  values diminished with distance for all seven brain states, the more similar a brain state was to anatomical connectivity, the faster the correlations decayed with distance ( $\beta$  value = -0.50;  $R^2 = 0.86$ ;  $P = 0.002$ ).

**Average Lifetime of Each Brain State during Ketamine Anesthesia.** The average lifetime of each brain state was also analyzed (Supplemental Digital Content, supplementary fig. 2A, <http://links.lww.com/ALN/B756>). With ketamine anesthesia, the average duration of brain state 7 increased compared to the awake state (Supplemental Digital Content, supplementary fig. 2A, <http://links.lww.com/ALN/B756>; bootstrap analysis; awake *vs.* ketamine anesthesia,  $P < 0.0001$ ).

### Dynamical Connectivity Results during Sevoflurane

Sevoflurane data were analyzed in the same manner. Again, the extracted seven brain states (fig. 3A) were ranked according to their similarity to the CoCoMac structural connectivity matrix (figs. 3 and 5; Supplemental Digital Content, supplementary figs. 2, 5, 6, <http://links.lww.com/ALN/B756>)<sup>27</sup>. In the awake state, with the same previous set of data now clustered with

the sevoflurane data, most brain states (except brain state 4) had a similar probability of occurrence, and these probabilities were not modulated by the structural connectivity/functional correlation similarity ( $\beta$  value = -0.17;  $R^2 = 0.02$ ;  $P = 0.75$ ; fig. 3, D and E). During sevoflurane anesthesia (moderate or deep), the brain states probability distribution was altered (fig. 3, D and F). Brain states 1, 2, and 3 disappeared during sevoflurane anesthesia, and the more similar a brain state was to the anatomical connectivity, the more probable it became during sevoflurane anesthesia (moderate sevoflurane sedation  $\beta$  value = 1.57;  $R^2 = 0.70$ ;  $P = 0.019$ ; deep sevoflurane anesthesia  $\beta$  value = 1.84;  $R^2 = 0.51$ ;  $P = 0.07$ ). The change in the brain state composition was significantly altered by sevoflurane anesthesia (ANOVA mean rank expressed as rounded rank: awake = 4 [mean, 3.91 ± 0.91], moderate sevoflurane sedation = 6 [mean, 5.98 ± 0.61], deep sevoflurane anesthesia = 6 [mean, 6.40 ± 0.72];  $F_{(2,69)} = 29.56$ ,  $P < 0.0001$ ). As previously seen for ketamine anesthesia, brain state 7 became dominant (ANOVA state 7 probability; awake = 0.31 [SD, 0.18]; moderate sevoflurane sedation = 0.53 [SD, 0.21]; deep sevoflurane anesthesia = 0.71 [SD, 0.27];  $F_{(2,69)} = 6.17$ ,  $P < 0.005$ ; fig. 4D).

The SD of the distribution of functional correlations increased as the similarity score decreased ( $\beta$  value = -2.32;  $R^2 = 0.46$ ,  $P = 0.09$ ). As already demonstrated for ketamine anesthesia, the distribution of  $z$  values of brain state 7 denoted low and sparse correlations, while the distribution for brain state 1 attested to the presence of strong functional correlations and anticorrelations (fig. 3H).

For brain state 1, dense strong positive and negative correlations were detected even for very distant pairs of nodes (figs. 3I and 5; Supplemental Digital Content, supplementary fig. 6, <http://links.lww.com/ALN/B756>). Brain state 7 had a predominance of short-range correlations, and functional correlations fell to zero as distance increased (figs. 3J and 5; Supplemental Digital Content, supplementary fig. 6, <http://links.lww.com/ALN/B756>). While  $z$  values reduced with distance for all the 7 brain states, the more similar a brain state was to anatomical connectivity, the faster the correlations declined with distance ( $\beta$  value = -0.45;  $R^2 = 0.73$ ;  $P = 0.01$ ).

**Average Lifetime of Each Brain State during Sevoflurane Anesthesia.** With sevoflurane, the average duration of brain state 7 increased only during deep sevoflurane anesthesia (Supplemental Digital Content, supplementary fig. 2B, <http://links.lww.com/ALN/B756>; bootstrap analysis; awake *vs.* moderate sevoflurane sedation,  $P < 0.0001$ ; awake *vs.* deep sevoflurane anesthesia,  $P < 0.0001$ ). These results observed with ketamine and sevoflurane are in line with our previous findings with propofol anesthesia.<sup>4</sup>

### Dynamical Connectivity Results during Anesthesia

In a final analysis, we pooled all the data and applied the k-means clustering algorithm to the data from the awake state, ketamine (deep), sevoflurane (moderate, deep), and propofol (moderate, deep) anesthesia (fig. 5, Supplemental

Digital Content, supplementary figs. 5, 6, <http://links.lww.com/ALN/B756>). The probability distribution of brain states was reshaped during all anesthetics (regression analysis; awake state:  $\beta$  value =  $-0.77$ ;  $R^2 = 0.14$ ;  $P = 0.41$ ; ketamine anesthesia:  $\beta$  value =  $1.84$ ;  $R^2 = 0.57$ ;  $P = 0.05$ ; moderate propofol anesthesia:  $\beta$  value =  $1.87$ ;  $R^2 = 0.47$ ;  $P = 0.09$ ; deep propofol anesthesia:  $\beta$  value =  $1.78$ ;  $R^2 = 0.55$ ;  $P = 0.057$ ; moderate sevoflurane sedation:  $\beta$  value =  $1.05$ ;  $R^2 = 0.72$ ;  $P = 0.015$ ; deep sevoflurane anesthesia:  $\beta$  value =  $1.65$ ;  $R^2 = 0.61$ ;  $P = 0.038$ ).

The change in brain state composition was also altered by all anesthetics (ANOVA rounded rank: awake = 4 [mean,  $3.58 \pm 1.03$ ]; ketamine anesthesia = 6 [mean,  $6.10 \pm 0.32$ ]; moderate propofol anesthesia = 6 [mean,  $6.15 \pm 0.76$ ]; deep propofol anesthesia = 6 [mean,  $6.16 \pm 0.46$ ]; moderate sevoflurane sedation = 5 [mean,  $5.10 \pm 0.81$ ]; deep sevoflurane anesthesia = 6 [mean,  $5.81 \pm 1.11$ ];  $F_{(5,146)} = 35.01$ ,  $P < 0.0001$ ).

Remarkably, brain state 1 was exclusively found in the repertoire of the awake state, while brain state 7 was predominant during anesthesia regardless of the pharmacologic agent (ketamine, sevoflurane, propofol; ANOVA state 7 probability; awake = 0.32 [SD, 0.17]; ketamine anesthesia = 0.61 [SD, 0.13]; moderate propofol anesthesia = 0.67 [SD, 0.24]; deep propofol anesthesia = 0.58 [SD, 0.18]; moderate sevoflurane sedation = 0.31 [SD, 0.19]; deep sevoflurane anesthesia = 0.53 [SD, 0.28];  $F_{(5,146)} = 10.74$ ,  $P < 0.0001$ ).

**Dynamical Functional Correlations in the Macaque Global Neuronal Workspace.** To further characterize the functional brain states of our dynamic cortical analysis, we measured functional correlations among global neuronal workspace nodes in each of the identified brain states (fig. 5; Supplemental Digital Content, supplementary fig. 6, <http://links.lww.com/ALN/B756>). Our data show that frontal eye fields, posterior cingulate, and parietal cortex express a striking difference between the most “flexible” brain state (*i.e.*, state 1) and the most “rigid” brain state (*i.e.*, state 7), with a high functional correlation between global neuronal workspace areas in state 1 and low or no correlations in state 7 (fig. 5, A, E, and F).

## Discussion

In this study, we found that three distinct anesthetics profoundly affected the dynamics of cortical brain activity patterns, with the functional correlation maps becoming very similar to the anatomical connectivity map, whatever the initial molecular mechanism.<sup>34</sup> This common mechanism relates to the relationship between functional brain configurations of dynamic-resting state and the underlying anatomical connectivity structure, as we previously demonstrated for propofol-induced anesthesia.<sup>4</sup> Here we generalize our previous finding and show that it provides a common brain signature of anesthesia-induced loss of consciousness. Anesthetics massively alter cortical activity by biasing

spontaneous fluctuations of cortical activity to a “rigid” brain configuration that is highly shaped by brain anatomy and by suppressing the “flexible” brain configurations that form a rich repertoire of brain states during the conscious condition. During anesthesia, the cluster of dynamic brain configurations is dominated by brain states with low functional correlations among prefrontal, parietal, and cingular cortices that form the global neuronal workspace nodes.

## Anesthesia Endpoint

Several studies used functional neuroimaging (electroencephalography and/or functional magnetic resonance imaging) to identify the brain signature of anesthesia, also called the “anesthetic endpoint,”<sup>1</sup> which is an information-processing endpoint. Stemming from these approaches, different mechanistic hypotheses emerged, including a functional disconnection between frontal and parietal cortices, an impairment in thalamocortical functional correlation, and an extinction of the cortical top-down feedback system.<sup>1</sup>

In our study, by clustering the functional magnetic resonance imaging resting-state data, we could delineate seven clusters, which corresponded to resting-state brain functional configurations or brain states. This clustering reveals a fundamental subdivision of cortical activity in the macaque brain that is consistent across conscious states. The increase of similarity between the brain functional configurations and the brain structure during anesthesia that we observed could explain the reported shift toward higher stability of brain intrinsic dynamics during anesthesia.<sup>35</sup> The functional dynamic in the resting state that we describe is common to all tested anesthetics, making it an anesthesia endpoint. Determining whether this endpoint is causal or not will require additional studies with selective pharmacologic,<sup>36</sup> electrical, or optical<sup>37</sup> manipulation of large brain networks that aim at reversing the loss of consciousness while keeping anesthetic pharmacologic administration.

## Mechanisms of Anesthesia-induced Loss of Consciousness

How can the predominance of “rigid” resting-state brain configurations explain the loss of consciousness during anesthesia? The assumption of temporal stationarity, implicit in many resting-state studies that compute functional correlations by averaging over a long period, fails to provide a complete description of the brain at rest. It leaves aside the important fact that in the conscious brain, functional correlations constantly change and exhibit complex temporal dynamics (see also Tononi *et al.*<sup>38</sup>). The conscious resting-state actually comprises a great variety of brain states that last for a few seconds and constantly wax and wane, in parallel with the subject’s psychologic state (for example, mind wandering).<sup>39</sup> These conscious states are naturally dependent on the preexisting anatomical connectivity, yet they selectively mobilize only a subset of the existing anatomical brain

networks. Our present and previous<sup>4</sup> results suggest that the more similar a functional state is to the anatomical connectivity matrix, the more probable it is to remain present during anesthesia (ketamine, sevoflurane, or propofol anesthesia; Supplemental Digital Content, supplementary fig. 5, <http://links.lww.com/ALN/B756>).

Characteristic of the awake state is the presence of negative correlations, suggesting an orchestrated dynamic of engaging and disengaging antagonistic networks, a characteristic that diminishes or disappears when the animal is anesthetized. This higher temporal variability may indicate a larger dynamic range of possible responses to incoming stimuli.<sup>40</sup> When variability is missing, the brain has little capacity to explore its state space, leading to an increased possibility that the system remains rigidly in a single state<sup>41</sup> and making spontaneous state-to-state transitions less probable.<sup>42</sup> Using auditory functional magnetic resonance imaging, we previously demonstrated that higher-order sequence violation activates a prefrontoparietocingular network in the awake state, which is completely suppressed during ketamine anesthesia and significantly disorganized during propofol anesthesia.<sup>6</sup> The disruption of higher-order functional cortical networks in parietal, prefrontal, and cingular cortices is key to induce loss of consciousness, probably through impoverishment of high-complexity resting-state configurations.

### **Interaction Among Frontal, Parietal, and Cingular Cortices during Anesthesia**

There is now strong evidence that anesthesia results in a decrease of frontoparietal functional correlation during ketamine,<sup>20</sup> propofol,<sup>7</sup> and sevoflurane.<sup>13,14</sup> In our study, we measured the corticocortical effects of ketamine, sevoflurane, and propofol anesthesia and found that all anesthetics preserved long-range stationary connections but created a drop in positive correlations and negative correlations compared to the awake state (although the effect on negative correlations was less important with sevoflurane). Those findings are consistent with the hypothesis that a disruption of long-distance corticocortical networks may explain the anesthesia-induced loss of consciousness.<sup>15,43,44</sup> They are also in agreement with several theories of consciousness suggesting that distributed functional networks sustain consciousness and that changes of these networks induce loss of consciousness.<sup>16,45</sup> Moreover, it has been suggested that there is a sort of “push–pull” relationship between activity in the anterior prefrontal and posterior sensory cortices, such that an intensive sensory activation decreases prefrontal cortex activity.<sup>46</sup> This model fits with our observations during anesthesia, suggesting that a lack of prefrontal feedback during anesthesia may be responsible for an increase in sensory activity (fig. 4B). For simplicity, the present work only measured correlation, which is a symmetrical and bidirectional measure of interactions between brain regions. To confirm this interpretation, future studies should attempt to perform a directional analysis, for instance with Granger causality or

other information-based measures,<sup>47</sup> to selectively dissect top-down from bottom-up information processing in awake and anesthetized macaques.

Finally, our data are consistent with previous work<sup>3,48,49</sup> showing that functional correlation decreased in the default mode network, particularly among the prefrontal, anterior cingulate, and the posterior cingulate cortices during all the anesthetic states, as compared to the awake state (fig. 4, A–D, F). It should be noted that our study examined a cortical correlate of anesthesia-induced loss of consciousness, independently from direct measurement of deep brain nuclei activity. The literature shows that ketamine and sevoflurane have opposite effects on thalamocortical activity. Under ketamine sedation, thalamocortical functional correlation is relatively preserved<sup>50</sup> or even increased.<sup>51</sup> Sevoflurane decreases thalamocortical functional correlation,<sup>49</sup> possibly because of a hyperpolarization of thalamic neurons during anesthesia.<sup>52</sup> The anesthesia “thalamic switch” hypothesis,<sup>53</sup> therefore, remains controversial, and several studies show that anesthesia-induced loss of consciousness is more associated with an impairment of cortical function than with an alteration of thalamic activity.<sup>7,54</sup> Finally, it has been demonstrated that disconnecting the prefrontal cortex from its thalamic inputs does not impair consciousness. Interestingly, we describe a common cortical mechanism for anesthesia-induced loss of consciousness that occurs independently from the differential modulation of the thalamic activity trigger by each anesthetic agent.

### **Global Neuronal Workspace during Anesthesia**

Our current findings derive from the study of resting-state functional magnetic resonance imaging in awake and anesthetized conditions. To link these findings to those we previously reported during auditory event-related functional magnetic resonance imaging,<sup>6,18</sup> we examined changes in functional correlation among representatives of the macaque global neuronal workspace areas that were previously found to respond to global novelty in the local-global paradigm<sup>18</sup> (*i.e.*, prefrontal cortex, parietal cortex, cingular cortex; figs. 4 and 5). Strikingly, the functional brain states that are predominant during anesthesia and are highly correlated with brain structure (*e.g.*, state 7) are characterized by low frontoparietal functional correlation, whereas those that are present only during the awake state (*e.g.*, state 1) are characterized by strong intervoxel correlations between prefrontal, parietal, and cingular cortices (figs. 4 and 5). Our data show that the dynamic resting-state clusters, although determined in a hypothesis-free, unsupervised manner, correspond to strong differences in frontoparietal functional correlation configurations, in good agreement with the global neuronal workspace theory.

### **Limitations of the Study**

One of the potential limitations of our study relates to the sevoflurane study as the induction was performed with ketamine. This initial ketamine injection was performed, as it is

challenging to induce anesthesia with sevoflurane in nonhuman primates, because of the lack of cooperation of the animal. However, this should not have affected our sevoflurane study significantly. In fact, we only analyzed the sevoflurane data acquired after 80 min of the ketamine induction. Schroeder *et al.*<sup>20</sup> demonstrated that the bandpower structure of the macaque cortical activity shifted quickly after a single ketamine injection and mostly recovered 80 min later. Another potential limitation of this study is that we used functional magnetic resonance imaging signal, which measures neuronal activity in an indirect manner, through local hemodynamic and metabolic changes. However, previous work performed in macaque monkeys could validate the strong correlation between neuronal activity and functional magnetic resonance imaging signal, including during different anesthetics.<sup>55</sup> Furthermore, it has been demonstrated that isoflurane dosage did not affect local field potentials to forepaw stimulation, but it altered local hemodynamic and neurovascular coupling in a dose-dependent manner.<sup>56</sup> However, this discrepancy was not observed in a resting-state study that combined functional magnetic resonance imaging and local field potentials recording.<sup>57</sup>

### Conclusions

Our results suggest that the temporal dynamics of spontaneous brain activity and its departure from rigid anatomical routes are altered during ketamine and sevoflurane anesthesia, just as previously observed with propofol anesthesia.<sup>4</sup> The loss of consciousness is systematically accompanied by a shift in dynamical functional correlation, leading to a rigid brain configuration during anesthesia, characterized by a loss of long-distance intracortical correlations within a global workspace network that includes prefrontal, parietal, and cingulate cortices. Future work should probe whether this signature also generalizes to other conditions such as coma, vegetative state, or epilepsy.

### Acknowledgments

The authors thank Wilfried Pianezzola for help with animal experiments; Alexis Amadon, Ph.D., Hauke Kolster, Ph.D., Laurent Larivière, Jérémy Bernard, Eric Giacomini, Michel Luong, Ph.D., Edouard Chazel, and the NeuroSpin magnetic resonance imaging and informatics teams for help with imaging tools; Christophe Joubert, D.V.M., and Jean-Marie Helies, D.V.M., for animal facilities; and Jean-Robert Deverre, Pharm.D., for administrative support, Commissariat à l'Énergie atomique et aux Énergies alternatives, Direction de la recherche fondamentale (CEA DRF/Joliot).

### Research Support

This work was supported by Institut National de la Santé et de la Recherche Médicale, the Inserm Avenir program (Paris, France; to Dr. Jarraya), Commissariat à l'Énergie Atomique (Gif-sur-Yvette, France), Collège de France (Paris, France), ERC Grant NeuroConsc (European Commission, Brussels, Belgium; to Dr. Dehaene), and Foundation Bettencourt-Schueller (Paris, France).

### Competing Interests

The authors declare no competing interests.

### Correspondence

Address correspondence to Dr. Jarraya: CEA Paris-Saclay, NeuroSpin, Bat 145, 91191 Gif-sur-Yvette, France. bechir.jarraya@cea.fr. Information on purchasing reprints may be found at [www.anesthesiology.org](http://www.anesthesiology.org) or on the masthead page at the beginning of this issue. ANESTHESIOLOGY's articles are made freely accessible to all readers, for personal use only, 6 months from the cover date of the issue.

### References

- Hudetz AG, Mashour GA: Disconnecting consciousness: Is there a common anesthetic end point? *Anesth Analg* 2016; 123:1228–40
- Horovitz SG, Braun AR, Carr WS, Picchioni D, Balkin TJ, Fukunaga M, Duyn JH: Decoupling of the brain's default mode network during deep sleep. *Proc Natl Acad Sci USA* 2009; 106:11376–81
- Boveroux P, Vanhaudenhuyse A, Bruno MA, Noirhomme Q, Lauwick S, Luxen A, Degueldre C, Plenevaux A, Schnakers C, Phillips C, Brichant JF, Bonhomme V, Maquet P, Greicius MD, Laureys S, Boly M: Breakdown of within- and between-network resting state functional magnetic resonance imaging connectivity during propofol-induced loss of consciousness. *ANESTHESIOLOGY* 2010; 113:1038–53
- Barttfeld P, Uhrig L, Sitt JD, Sigman M, Jarraya B, Dehaene S: Signature of consciousness in the dynamics of resting-state brain activity. *Proc Natl Acad Sci USA* 2015; 112:887–92
- Ferrarelli F, Massimini M, Sarasso S, Casali A, Riedner BA, Angelini G, Tononi G, Pearce RA: Breakdown in cortical effective connectivity during midazolam-induced loss of consciousness. *Proc Natl Acad Sci USA* 2010; 107:2681–6
- Uhrig L, Janssen D, Dehaene S, Jarraya B: Cerebral responses to local and global auditory novelty under general anesthesia. *Neuroimage* 2016; 141:326–40
- Boly M, Moran R, Murphy M, Boveroux P, Bruno MA, Noirhomme Q, Ledoux D, Bonhomme V, Brichant JF, Tononi G, Laureys S, Friston K: Connectivity changes underlying spectral EEG changes during propofol-induced loss of consciousness. *J Neurosci* 2012; 32:7082–90
- Greicius MD, Kiviniemi V, Tervonen O, Vainionpää V, Alahuhta S, Reiss AL, Menon V: Persistent default-mode network connectivity during light sedation. *Hum Brain Mapp* 2008; 29:839–47
- Guldenmund P, Demertzi A, Boveroux P, Boly M, Vanhaudenhuyse A, Bruno MA, Gosseries O, Noirhomme Q, Brichant JF, Bonhomme V, Laureys S, Soddu A: Thalamus, brainstem and salience network connectivity changes during propofol-induced sedation and unconsciousness. *Brain Connect* 2013; 3:273–85
- Peduto VA, Concas A, Santoro G, Biggio G, Gessa GL: Biochemical and electrophysiologic evidence that propofol enhances GABAergic transmission in the rat brain. *ANESTHESIOLOGY* 1991; 75:1000–9
- Anis NA, Berry SC, Burton NR, Lodge D: The dissociative anaesthetics, ketamine and phencyclidine, selectively reduce excitation of central mammalian neurones by N-methyl-aspartate. *Br J Pharmacol* 1983; 79:565–75
- Wu J, Harata N, Akaike N: Potentiation by sevoflurane of the gamma-aminobutyric acid-induced chloride current in acutely dissociated CA1 pyramidal neurones from rat hippocampus. *Br J Pharmacol* 1996; 119:1013–21
- Ranft A, Golkowski D, Kiel T, Riedl V, Kohl P, Rohrer G, Pientka J, Berger S, Thul A, Maurer M, Preibisch C, Zimmer C, Mashour GA, Kochs EF, Jordan D, Ilg R: Neural correlates of sevoflurane-induced unconsciousness identified

- by simultaneous functional magnetic resonance imaging and electroencephalography. *ANESTHESIOLOGY* 2016; 125:861–72
14. Palanca BJ, Mitra A, Larson-Prior L, Snyder AZ, Avidan MS, Raichle ME: Resting-state functional magnetic resonance imaging correlates of sevoflurane-induced unconsciousness. *ANESTHESIOLOGY* 2015; 123:346–56
  15. Lee U, Ku S, Noh G, Baek S, Choi B, Mashour GA: Disruption of frontal-parietal communication by ketamine, propofol, and sevoflurane. *ANESTHESIOLOGY* 2013; 118:1264–75
  16. Dehaene S, Kerszberg M, Changeux JP: A neuronal model of a global workspace in effortful cognitive tasks. *Proc Natl Acad Sci USA* 1998; 95:14529–34
  17. Baars BJ, Laureys S: One, not two, neural correlates of consciousness. *Trends Cogn Sci* 2005; 9:269; author reply 270
  18. Uhrig L, Dehaene S, Jarraya B: A hierarchy of responses to auditory regularities in the macaque brain. *J Neurosci* 2014; 34:1127–32
  19. Absalom A, Kenny G: 'Paedfusor' pharmacokinetic data set. *Br J Anaesth* 2005; 95:110
  20. Schroeder KE, Irwin ZT, Gaidica M, Nicole Bentley J, Patil PG, Mashour GA, Chestek CA: Disruption of corticocortical information transfer during ketamine anesthesia in the primate brain. *Neuroimage* 2016; 134:459–65
  21. Schüttler J, Stanski DR, White PF, Trevor AJ, Horai Y, Verotta D, Sheiner LB: Pharmacodynamic modeling of the EEG effects of ketamine and its enantiomers in man. *J Pharmacokinetic Biopharm* 1987; 15:241–53
  22. Pinault D: N-methyl D-aspartate receptor antagonists ketamine and MK-801 induce wake-related aberrant gamma oscillations in the rat neocortex. *Biol Psychiatry* 2008; 63:730–5
  23. Feshchenko VA, Veselis RA, Reinsel RA: Propofol-induced alpha rhythm. *Neuropsychobiology* 2004; 50:257–66
  24. Murphy M, Bruno MA, Riedner BA, Boveroux P, Noirhomme Q, Landsness EC, Brichant JF, Phillips C, Massimini M, Laureys S, Tononi G, Boly M: Propofol anesthesia and sleep: a high-density EEG study. *Sleep* 2011; 34:283–91A
  25. Purdon PL, Pierce ET, Mukamel EA, Prerau MJ, Walsh JL, Wong KF, Salazar-Gomez AF, Harrell PG, Sampson AL, Cimenser A, Ching S, Kopell NJ, Tavares-Stoeckel C, Habeeb K, Merhar R, Brown EN: Electroencephalogram signatures of loss and recovery of consciousness from propofol. *Proc Natl Acad Sci USA* 2013; 110:E1142–51
  26. Gugino LD, Chabot RJ, Pritchep LS, John ER, Formanek V, Aglio LS: Quantitative EEG changes associated with loss and return of consciousness in healthy adult volunteers anesthetized with propofol or sevoflurane. *Br J Anaesth* 2001; 87:421–8
  27. Bakker R, Wachtler T, Diesmann M: CoCoMac 2.0 and the future of tract-tracing databases. *Front Neuroinform* 2012; 6:30
  28. Kötter R, Wanke E: Mapping brains without coordinates. *Philos Trans R Soc Lond B Biol Sci* 2005; 360:751–66
  29. Allen EA, Damaraju E, Blis SM, Erhardt EB, Eichele T, Calhoun VD: Tracking whole-brain connectivity dynamics in the resting state. *Cereb Cortex* 2014; 24:663–76
  30. Hutchison RM, Womelsdorf T, Gati JS, Everling S, Menon RS: Resting-state networks show dynamic functional connectivity in awake humans and anesthetized macaques. *Hum Brain Mapp* 2013; 34:2154–77
  31. Lloyd S: Least squares quantization in PCM. *IEEE Trans Inf Theory* 1982; 28:129–37
  32. Efron B, Tibshirani RJ: *An Introduction to the Bootstrap*. New York, Chapman and Hall, 1994
  33. Vincent JL, Patel GH, Fox MD, Snyder AZ, Baker JT, Van Essen DC, Zempel JM, Snyder LH, Corbetta M, Raichle ME: Intrinsic functional architecture in the anaesthetized monkey brain. *Nature* 2007; 447:83–6
  34. Uhrig L, Dehaene S, Jarraya B: Cerebral mechanisms of general anesthesia. *Ann Fr Anesth Reanim* 2014; 33:72–82
  35. Solovey G, Alonso LM, Yanagawa T, Fujii N, Magnasco MO, Cecchi GA, Proekt A: Loss of consciousness is associated with stabilization of cortical activity. *J Neurosci* 2015; 35:10866–77
  36. Alkire MT, McReynolds JR, Hahn EL, Trivedi AN: Thalamic microinjection of nicotine reverses sevoflurane-induced loss of righting reflex in the rat. *ANESTHESIOLOGY* 2007; 107: 264–72
  37. Liu J, Lee HJ, Weitz AJ, Fang Z, Lin P, Choy M, Fisher R, Pinsky V, Tolpygo A, Mitra P, Schiff N, Lee JH: Frequency-selective control of cortical and subcortical networks by central thalamus. *Elife* 2015; 4:e09215
  38. Tononi G, Boly M, Massimini M, Koch C: Integrated information theory: From consciousness to its physical substrate. *Nat Rev Neurosci* 2016; 17:450–61
  39. Kucyi A: Just a thought: How mind-wandering is represented in dynamic brain connectivity. *Neuroimage* 2017; S1053-8119:30569–4
  40. Huang Z, Zhang J, Wu J, Qin P, Wu X, Wang Z, Dai R, Li Y, Liang W, Mao Y, Yang Z, Zhang J, Wolff A, Northoff G: Decoupled temporal variability and signal synchronization of spontaneous brain activity in loss of consciousness: An fMRI study in anesthesia. *Neuroimage* 2016; 124(Pt A):693–703
  41. Deco G, Jirsa V, McIntosh AR, Sporns O, Kötter R: Key role of coupling, delay, and noise in resting brain fluctuations. *Proc Natl Acad Sci USA* 2009; 106:10302–7
  42. Garrett DD, Samanez-Larkin GR, MacDonald SW, Lindenberger U, McIntosh AR, Grady CL: Moment-to-moment brain signal variability: A next frontier in human brain mapping? *Neurosci Biobehav Rev* 2013; 37:610–24
  43. Monti MM, Lutkenhoff ES, Rubinov M, Boveroux P, Vanhauzenhuyse A, Gosseries O, Bruno MA, Noirhomme Q, Boly M, Laureys S: Dynamic change of global and local information processing in propofol-induced loss and recovery of consciousness. *PLoS Comput Biol* 2013; 9:e1003271
  44. Blain-Moraes S, Lee U, Ku S, Noh G, Mashour GA: Electroencephalographic effects of ketamine on power, cross-frequency coupling, and connectivity in the alpha bandwidth. *Front Syst Neurosci* 2014; 8:114
  45. Oizumi M, Albantakis L, Tononi G: From the phenomenology to the mechanisms of consciousness: Integrated Information Theory 3.0. *PLoS Comput Biol* 2014; 10:e1003588
  46. Golland Y, Golland P, Bentin S, Malach R: Data-driven clustering reveals a fundamental subdivision of the human cortex into two global systems. *Neuropsychologia* 2008; 46:540–53
  47. Seth AK, Barrett AB, Barnett L: Granger causality analysis in neuroscience and neuroimaging. *J Neurosci* 2015; 35:3293–7
  48. Schrouff J, Perlberg V, Boly M, Marrelec G, Boveroux P, Vanhauzenhuyse A, Bruno MA, Laureys S, Phillips C, Péligrini-Issac M, Maquet P, Benali H: Brain functional integration decreases during propofol-induced loss of consciousness. *Neuroimage* 2011; 57:198–205
  49. Huang Z, Wang Z, Zhang J, Dai R, Wu J, Li Y, Liang W, Mao Y, Yang Z, Holland G, Zhang J, Northoff G: Altered temporal variance and neural synchronization of spontaneous brain activity in anesthesia. *Hum Brain Mapp* 2014; 35:5368–78
  50. Bonhomme V, Vanhauzenhuyse A, Demertzi A, Bruno MA, Jaquet O, Bahri MA, Plenevaux A, Boly M, Boveroux P, Soddu A, Brichant JF, Maquet P, Laureys S: Resting-state network-specific breakdown of functional connectivity during ketamine alteration of consciousness in volunteers. *ANESTHESIOLOGY* 2016; 125:873–88
  51. Hofflich A, Hahn A, Kublbock M, Kranz GS, Vanicek T, Windischberger C, Saria A, Kasper S, Winkler D, Lanzenberger R: Ketamine-induced modulation of the thalamo-cortical network in healthy volunteers as a model for schizophrenia. *Int J Neuropsychopharmacol* 2015; 18:pyv040

52. Meuth SG, Budde T, Kanyshkova T, Broicher T, Munsch T, Pape HC: Contribution of TWIK-related acid-sensitive K<sup>+</sup> channel 1 (TASK1) and TASK3 channels to the control of activity modes in thalamocortical neurons. *J Neurosci* 2003; 23:6460–9
53. Alkire MT, Hudetz AG, Tononi G: Consciousness and anesthesia. *Science* 2008; 322:876–80
54. Velly LJ, Rey MF, Bruder NJ, Gouvitsos FA, Witjas T, Regis JM, Peragut JC, Gouin FM: Differential dynamic of action on cortical and subcortical structures of anesthetic agents during induction of anesthesia. *ANESTHESIOLOGY* 2007; 107:202–12
55. Logothetis NK, Pauls J, Augath M, Trinath T, Oeltermann A: Neurophysiological investigation of the basis of the fMRI signal. *Nature* 2001; 412:150–7
56. Masamoto K, Fukuda M, Vazquez A, Kim SG: Dose-dependent effect of isoflurane on neurovascular coupling in rat cerebral cortex. *Eur J Neurosci* 2009; 30:242–50
57. Pan WJ, Thompson G, Magnuson M, Majeed W, Jaeger D, Keilholz S: Broadband local field potentials correlate with spontaneous fluctuations in functional magnetic resonance imaging signals in the rat somatosensory cortex under isoflurane anesthesia. *Brain Connect* 2011; 1:119–31